Reimplementing Fairness by Learning Orthogonal Disentangled Representations

Siem Teusink (11433175)
University of Amsterdam
Faculty of Science

Pim Meerdink (11644095)
University of Amsterdam
Faculty of Science

Paul Lodder (10991735)
University of Amsterdam
Faculty of Science

Jeroen Jagt (11834684)
University of Amsterdam
Faculty of Science

Reproducibility Summary

Scope of Reproducibility

Sarhan et al. [2020] propose a method of learning representations that can be used in downstream tasks, yet that are independent of certain sensitive attributes, such as race or sex. The learned representations can be considered "fair" as they are independent of sensitive attributes. The authors report results on five different datasets, which most notably include (1) the ability of the representations to be used for downstream tasks (target prediction accuracy) and (2) the extent to which sensitive information is present in these representations (sensitive prediction accuracy).

In this text we report and compare the obtained results as well as highlight any difficulties encountered in reproducing the reference paper by Sarhan et al. [2020].

Methodology

As there was no openly available code base, we re-implemented the work. We included scripts to automatically download the required data, designed the dataloaders, and implemented the models as described in the reference paper. Code is available `https://github.com/paulodder/fact2021`.

Results

We were able to reproduce some of the results of the paper, but a significant part of our results was inconsistent with the findings of Sarhan et al. [2020]. For some of the simpler datasets we found similar patterns, but for the more complex tasks the models training became unstable, leading to results that varied significantly across random seeds. This made reproduction infeasible.

What was easy and what was difficult

Conceptually, the paper was interesting and, given some prior knowledge on Variational Autoencoders and the math involved, it was also relatively straightforward to understand.

The most difficult aspect of the project was dealing with missing information. Many essential implementation details were missing, and there were inconsistencies in the pseudo code provided. Resolving these issues provided significant difficulties.

Communication with original authors

Various emails were exchanged with the original authors, in which we received explanation about unclear aspects of the paper. In general the authors were very helpful, but despite the fact that a few emails were exchanged, some aspect of the paper still remained unclear.

1 Introduction

A challenging problem in machine learning is learning representations that are fair with regards to a sensitive attribute present in the original samples. A common definition of fairness in this context is that the model's output is statistically independent from the sensitive attribute [Xie et al., 2017, Roy and Boddeti, 2019a, Quadrianto et al., 2019, Barocas, 2019]. Sarhan et al. [2020] proposed a new way to learn fair representations that are invariant towards the sensitive attribute, but are still useful for the task at hand. The proposed method to achieve this invariability is to disentangle the latent representation into independent target and sensitive representations [Locatello et al., 2019]. As a proxy for independence, orthogonality is enforced between these individual representations. Furthermore, in order to prevent sensitive information leaking into the target representation, the model is trained to learn a target representation which is agnostic to the sensitive information, maximizing the entropy of our sensitive attribute given the target representation.

In order to consolidate the claims brought forth in the reference work of this report Sarhan et al. [2020], and to assess the reproducibility of this work, our research attempts to reproduce the achieved results by re-implementing the proposed method. In the next section, we specify the parts of the original work that we attempt to reproduce. In Section 3, we summarize the method as proposed by Sarhan et al. [2020] that we attempt to re-implement. In Section 4, we report the results we attain. Finally, in Section 5, we discuss the results, and we analyse the reproducibility of the reference work.

2 Scope of reproducibility

The reference work by Sarhan et al. [2020] works towards a method of generating embeddings of data which are useful for downstream tasks, while they remain invariant towards a particular (sensitive) feature. The efficacy of this proposed method is assessed using two evaluative questions. First, how well can the learned target representation be used in the target task? Second, to what degree is information which might reveal the sensitive attribute still present in the learned target representation?

In the reference work, a collection of three binary- and two multi-class classification tasks are considered for a total of five classification tasks, corresponding to five different datasets. For each of these tasks, a version of the proposed model is trained, and evaluated using two metrics: *target accuracy* and a *sensitive accuracy*. The target accuracy measures how well we are able to predict the target attribute based on the produced target representation, and the sensitive accuracy measures how well we are able to predict the sensitive attribute based on the target representation – note that we want the sensitive accuracy to be as low as possible, because this implies that the target representation is independent of the sensitive attribute. Both of these accuracies, for each of the five tasks at hand, are included in our reproduction.

Furthermore, an ablative study is conducted in the reference work, in which specific components of the loss function used to train the model are excluded (i.e., ablated), in order to observe the behaviour of the model and, in doing so, understand the role of each of these loss components within the training process. This ablative study, which entails the evaluation of the impact of five unique combinations of loss components, is performed on each of the five datasets, and is included in our reproduction.

Finally, the authors perform a sensitivity analysis on the hyperparameters that control the relative importance of two of the loss terms they used, for one of the five tasks. For each combination of these hyperparameters, the model is trained, and the resulting target and sensitive accuracies achieved are displayed on a heatmap. We include this sensitivity analysis in our reproduction.

3 Methodology

Since the code of the original implementation is not available, it is our goal to reproduce the method, based on all implementation details expounded in the reference work. The essential elements of the model are described in the next section. For a more detailed explanation, we refer the reader to the reference work Sarhan et al. [2020].

3.1 Model descriptions

Let $\mathcal{X}$ be the dataset and let $\boldsymbol{x} \in \mathbb{R}^D$ be a single input sample. Each sample has an associated target vector $\boldsymbol{y} \in \mathbb{R}^n$ and an associated sensitive attribute vector $\boldsymbol{s} \in \mathbb{R}^m$, with n and m classes respectively. In order to map $\boldsymbol{x}$ to two latent representations; a target latent representation $\boldsymbol{z}_T$ and a sensitive latent representation $\boldsymbol{z}_S$. This mapping is learned by an encoder, which is composed as follows: the first part of the encoder, which we denote $f(\boldsymbol{x}, \theta)$, is shared between the target and sensitive representation. The output of this shared encoder is fed through two separate encoders $q_{\theta_T}(\boldsymbol{z}_T|\boldsymbol{x})$ and $q_{\theta_S}(\boldsymbol{z}_S|\boldsymbol{x})$, which each output a distribution in the latent space, and from which we sample the target and sensitive representations respectively. Here, θ_T and θ_S denote the sets of trainable parameters for either encoder, and include the parameters for the shared encoder, which can be found by $\theta = \theta_T \cap \theta_S$.

The target label $\hat{\boldsymbol{y}}$ is then predicted by the target discriminator $q_{\phi_t}(\boldsymbol{y}|\boldsymbol{z}_T)$, based on the target representation $\boldsymbol{z}_T$. Similarly, the sensitive label $\hat{\boldsymbol{s}}$ is predicted by the sensitive discriminator $q_{\phi_S}(\boldsymbol{s}|\boldsymbol{z}_S)$, based on $\boldsymbol{z}_T$. The encoder and discriminators are trained in supervised fashion to minimize the following losses, which we call the representation losses:

$$\mathcal{L}_T(\theta_T, \phi_T) = KL(p(\boldsymbol{y}|\boldsymbol{x}) \parallel q_{\phi_t}(\hat{\boldsymbol{y}}|\boldsymbol{z}_T)) \tag{1}$$

$$\mathcal{L}_S(\theta_S^*, \phi_S) = KL(p(\boldsymbol{s}|\boldsymbol{x}) \parallel q_{\phi_S}(\hat{\boldsymbol{s}}|\boldsymbol{z}_S)) \tag{2}$$

Here $\theta_S^* = \theta_S \backslash \theta$. These losses are effectively equal to the cross-entropy between the predicted values for the targets and sensitive attributes and their actual values. Note that by backpropagating our sensitive representation loss through θ_S^*, we prevent the shared parameters θ from being updated twice.

To ensure that no sensitive information can leak into the target representation, we maximize the entropy of the sensitive attribute given the target representation, following Roy and Boddeti [2019a], Sarhan et al. [2020]. This is achieved by minimizing

$$\mathcal{L}_E(\phi_S, \theta_T) = KL(q_{\phi_S}(\boldsymbol{s}|\boldsymbol{z}_T) \parallel \mathcal{U}(\boldsymbol{s})) \tag{3}$$

Last, we want to ensure that there is some level of independence between the two representations. Ideally, we want the posterior $p(\boldsymbol{z}_T|\boldsymbol{x})$ to be statistically independent of $p(\boldsymbol{z}_S|\boldsymbol{x})$. Following Sarhan et al. [2020], we relax this independence requirement to the enforcing of two properties: one, a disentanglement property (i.e. independence across dimensions within a representation), and two, orthogonality between the two representations. To enforce these properties, we need to *estimate* the aforementioned posteriors (as they are intractable) using variational inference [Kingma and Welling, 2014]. The encoder network is be similar to the encoder of a Variational Auto-Encoder (VAE) model [Kingma and Welling, 2013], in that it outputs the means $(\boldsymbol{\mu}_T, \boldsymbol{\mu}_S)$ and covariance matrix diagonals $(\text{diag}(\boldsymbol{\sigma}_T), \text{diag}(\boldsymbol{\sigma}_S))$ for both latent distributions. We enforce disentanglement by only computing the diagonals of our covariance matrices and we enforce orthogonality by minimizing the KL divergence between each latent distribution with its prior, where we initialize the priors with orthogonal means: $\mathcal{L}_{z_T}(\theta_T) = KL(q_{\theta_T}(\boldsymbol{z}_T|\boldsymbol{x}) \parallel p(\boldsymbol{z}_T))$ and $\mathcal{L}_{z_S}(\theta_S) = KL(q_{\theta_S}(\boldsymbol{z}_S|\boldsymbol{x}) \parallel p(\boldsymbol{z}_S))$

Here $q_{\theta_T}(\boldsymbol{z}_T|\boldsymbol{x}) = \mathcal{N}(\boldsymbol{z}_T|\boldsymbol{\mu}_T, \text{diag}(\boldsymbol{\sigma}_T^2))$ and $q_{\theta_S}(\boldsymbol{z}_S|\boldsymbol{x}) = \mathcal{N}(\boldsymbol{z}_S|\boldsymbol{\mu}_S, \text{diag}(\boldsymbol{\sigma}_S^2))$.

We combine these two loss terms into a single term, which we call the *Orthogonal Disentangled (OD)* loss:

$$\mathcal{L}_{OD}(\theta_T, \theta_S) = \mathcal{L}_{z_T}(\theta_T) + \mathcal{L}_{z_S}(\theta_S)$$

We use the re-parameterization trick [Kingma and Welling, 2013] to sample from the approximated posterior distribution to obtain the latent representations, which can then be fed to the respective discriminators.

All of the aforementioned individual loss terms are further worked out in Appendix A. We combine all of them into one loss term and arrive at the following objective:

$$\underset{\theta_T, \theta_S, \phi_T, \phi_S}{argmin} \; \mathcal{L}_T(\theta_T, \phi_T) + \mathcal{L}_S(\theta_{S^*}, \phi_S) + : sarhan_sensitive_adult_E \mathcal{L}_E(\theta_T, \phi_S) + \lambda_{OD}\mathcal{L}_{OD}(\phi_T, \phi_S) \tag{4}$$

Here λ_{OD} and λ_E determine the relative importance of the OD loss and the entropy loss respectively. Additionally, we use two decay parameters, γ_{OD} and γ_E which allows us to change the weights of the aforementioned losses while training. These loss weights at epoch t during training are calculated as follows:

$$\lambda_{OD}^{(t)} = \lambda_{OD}^{(0)} \gamma_{OD}^{t/t_s} \tag{5}$$

$$\lambda_E^{(t)} = \lambda_E^{(0)} \gamma_E^{t/t_s} \tag{6}$$

Here t_s is the so-called *step-size* hyperparameter, and $\lambda_{OD}^{(0)}, \lambda_E^{(0)}$ are the initial loss weights. The entropy loss weight will be computed in the same way. $\lambda_{OD}^{(0)}, \lambda_E^{(0)}, \gamma_{OD}, \gamma_E$ and t_s are all hyperparameters that we need to set.

3.2 Datasets

In order to reproduce the results obtained by Sarhan et al. [2020] it was necessary to apply the model to five datasets. Below, we outline some basic properties of the datasets and we explain the sensitive and target attributes that are to be modeled. For detailed information about the datasets such as train/test splits, number of samples and dimensions we refer to Table 3 in the Appendix.

Tabular data

The Adult and German dataset were obtained from the UCI repository [Dua and Graff, 2017]. Both of these datasets contain census data, and include categorical and continuous attributes which contain information about the person's gender, education, and occupation. For both datasets, preprocessing consisted of representing categorical columns in a one-hot encoding, where missing values were explicitly encoded as a separate category, while continuous variables were left unchanged.

For the Adult dataset, the task is to predict whether a persons income exceeds $\$50,000$, and the sensitive attribute is gender. For the German dataset the task is to classify rows as having good or bad credit risk. Similar to the Adult dataset, the sensitive attribute is gender.

YaleB data

The Extended YaleB dataset was collected from the University of Toronto computer science department website Georghiades et al. [2000]. Specifically, the 'Cropped' version of the dataset was used [Lee et al., 2005], which contains grayscale images of 38 human faces under different lighting conditions. The task is to identify to which of the 38 humans an image corresponds. We constructed a sensitive attribute by clustering the illumination conditions into 5 clusters loosely corresponding to top left, bottom left, top right, bottom right and center. We defined these classes ourselves as we were unable to find detailed information on how this was done in the study by Sarhan et al. More details about the clustering of the illumination conditions can be found in the Appendix. Note that our majority class is not in line with the paper by Sarhan et al, who mention that a majority class classifier could attain 50% accuracy, in our case this is around 35%. Unfortunately, we were unable to find sufficient information to be able to replicate the ratios mentioned in the reference paper, and instead constructed our own sensitive attributes.

Our training dataset comprised of 190 images corresponding to one lighting position from each cluster, following [Sarhan et al., 2020, Louizos et al., 2015]. It is important to note that our testing dataset contained 2243 images, while the testing set in the reference work contained only 1096. The reason for this is unclear, as we used the full dataset, and found no mention of the omission of certain images in the reference paper.

CIFAR data

The CIFAR-10 and CIFAR-100 datasets were also collected from the University of Toronto computer science department website [Georghiades et al., 2000]. CIFAR-10 consists of colour images that are divided into 10 classes such as airplane, automobile and bird. For our purposes, we construct a new target attribute, one that denotes whether the subject of the image is alive or not, following [Roy and Boddeti, 2019a]. The sensitive attribute, then, is the original label of the image. The CIFAR-100 dataset is similar to CIFAR-10, except that images are categorized as one of 100 total fine-grained classes. These 100 fine classes are split into 20 coarse classes that cluster similar concepts into one category. For example: 'beaver', 'dolphin' and 'otter' all belong to the coarse class 'aquatic mammals' (c.f. [Roy and Boddeti, 2019b]). Here, the coarse class of an image is used as the target attribute, while its fine class is used as the sensitive attribute.

3.3 Implementation details

Following the paper of Sarhan et al. [2020], we implement the following networks for the several datasets. Note that, for every MLP mentioned below, ReLU's are used as (non-final) activation functions. For the CIFAR-10 and CIFAR-100 tasks, the encoder used was the ResNet-18 architecture [He et al., 2016].

3.4 Hyperparameters

Most used hyperparameters were taken directly from the reference work, or its supplement provided by Sarhan et al. However, optimal values for some hyperparameters were not reported, and thus, we empirically set these to values that seemed to result in satisfactory performance. We discuss which hyperparameters we were missing in Section 5, and report all hyperparameters that we used in the Appendix.

3.5 Experimental setup and code

Setup Reproducibility

Our implementation and instructions to run the code are available at `https://github.com/paulodder/fact2021`. The repository contains a folder `scripts` that contains all the scripts necessary to perform several tasks. All instructions for setting up are in the `README` and instructions for reproducing any of the numbers or figures reported in this text can be found in `produce_results.pdf` in the aforementioned repository.

Evaluation

Evaluation of the embeddings learned by our model is non trivial, as we must gather whether the embeddings adequately represent the data for the downstream task (e.g. classification of target attribute), while also ensuring that the embeddings contain no sensitive information. In order to quantitively evaluate our model after completing training, we train two classifiers. These classifiers use the test data that is embedded using our trained model in the target space.

The first classifier, known as the *target predictor* is trained to predict the target label from the target embeddings. In accordance with the reference paper, we evaluated the target predictor using accuracy as metric. The details of the target predictors used are reported in Table **??** in the Appendix. It is desirable that the target predictor performs as well as possible, as this means that the target embeddings embed the information necessary for the downstream task well.

The second classifier, known as the *sensitive predictor* is trained to predict the sensitive attribute from the target representation. For the sensitive predictor we use the exact same architecture and hyperparameters as for the sensitive discriminator. It is desirable that this classifier performs poorly, as we would like there to be no information pertaining to the sensitive attribute in our target embedding. As such, we would like the model to be as close to a 'majority classifier' as possible, where the model is forced to simply predict the majority label for each data row as it has no meaningful information with which to make a prediction about the sensitive attribute. Again, we use solely accuracy as evaluation metric.

Additional avenues of exploration

For the sake of completeness, we briefly report alternatives that were explored but did not yield improved results, and were therefore abandoned. None of the features described below were used to generate results.

In order to select the best performing model to evaluate, two independent selection mechanisms were implemented, but not used in the final experiments. (1) We attempted to select the best iteration of the proposed model (over all epochs) by keeping track of the version in which performance was best. We first defined performance as train target accuracy (higher is better). Later, to also take into account the extent of sensitive information leakage in the target representations, we also included the accuracy of predicting sensitive attributes based on target representations. (2) we attempted to select the best iteration of target and sensitive predictors during their training, again by tracking based on their performance. Here, performance was defined as test target accuracy. However, this augmentation was discarded as we were unsure whether this was implemented correctly, as results did not improve (even though it should, in theory).

For YaleB, various model architectures were implemented in an attempt to amend performance on this dataset. We experimented with variations in the dimensionality and number of hidden layers of the encoder and discriminators, activation functions (specifically, we tried `Tanh`), and the hyperparameters learning rate, max epochs, batch size, λ_{OD}, λ_E, γ_{OD}, and γ_E.

For CIFAR-10 and CIFAR-100, we experimented with freezing the ResNet-18 encoder (with the exception of the final, Linear layer, which was reinitialized), but despite faster training, the model's performance did not increase.

3.6 Computational Requirements

Table 1: The average run-time for each of the five datasets and their configurations.

Dataset	Adult	German	YaleB	CIFAR-10	CIFAR-100	Total
Average run-time (min.)	0.8	0.22	2	11	19	62
Number of epochs	2	15	30	30	55	-

We used Google Colab Pro to train our models, which supplies one `Tesla V100-SXM2-16GB` GPU, and 2 `Intel(R) Xeon(R) CPU @ 2.00GHz` CPUs. Average run-times are specified in Table 1. In order to train all models over various seeds for all results, this would be the estimated required run-time:

$$(3 * 62) + (5 * 5 * 62) + (2 * 8^2 * 5 * 0.8) = 4,296 \text{ minutes}$$

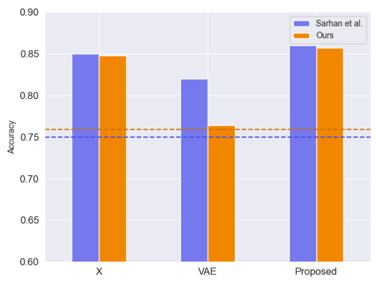

(a) Adult target accuracy

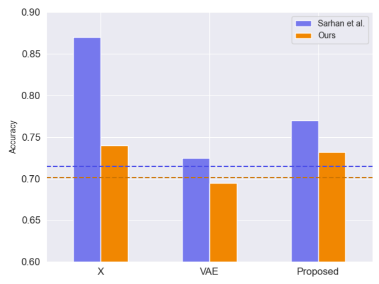

(b) German target accuracy

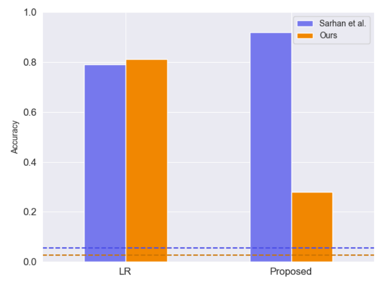

(c) YaleB target accuracy

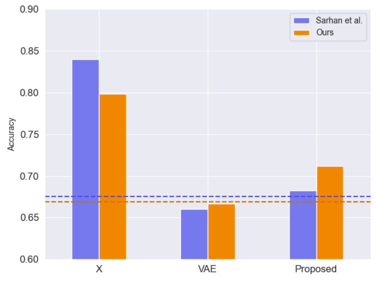

(d) Adult sensitive accuracy

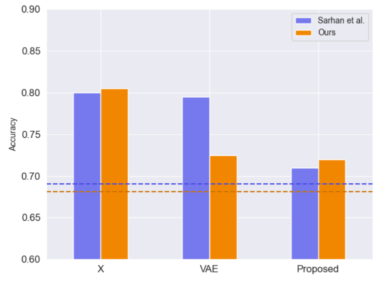

(e) German sensitive accuracy

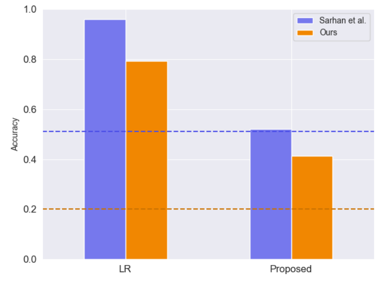

(f) YaleB sensitive accuracy

Figure 1: Performance of the proposed model, together with majority label classifier (denoted by the horizontal dashed line) and various other models for Adult, German, and YaleB datasets, compared between Sarhan et al. and our reproduction. The bars denoted by X correspond to direct use of the input data for our target prediction. Furthermore, a VAE was trained on the Adult and German datasets using MSE loss as reconstruction loss, and the accuracies denoted with 'VAE' correspond to the performance achieved by target and sensitive predictors trained on these VAE embeddings as input features. For YaleB, Logistic Regression was also performed on the raw data to predict the sensitive and target attributes, whose performance is denoted by 'LR'.

4 Results

To judge the reproducibility of the model proposed by Sarhan et al. [2020], we compare their results with those results we were able to attain using our implementation. First, we compare target and sensitive accuracy attained by training and evaluating the proposed model on each of the five datasets. Second, we compare the results of the ablative study. Finally, we make the same comparison for the sensitive study.

4.1 Results reproducing original paper

CIFAR-10 and CIFAR-100

Table 2: Results on CIFAR-10 and CIFAR-100 datasets

	CIFAR-10		CIFAR-100	
	Target Acc. ↑	Sensitive Acc. ↓	Target Acc. ↑	Sensitive Acc. ↓
Sarhan et al.	0.9725	0.1907	0.7074	0.1447
Ours	0.9582	0.3462	0.0500	0.0100

While we have been able to reproduce the CIFAR-10 target accuracy attained by Sarhan et al., the CIFAR-10 sensitive accuracy we attained is substantially higher than theirs, as displayed in Table 2. As for the CIFAR-100 dataset, our results strongly differed from those reported by Sarhan et al., as our model was not able to learn a representation that carried meaningful information, resulting in target and sensitive accuracies that are equal to accuracies attained by majority vote (see Table 2).

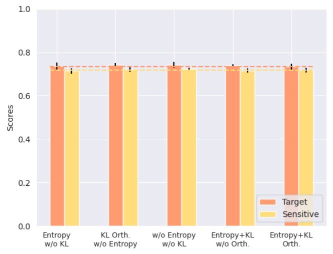

(a) German

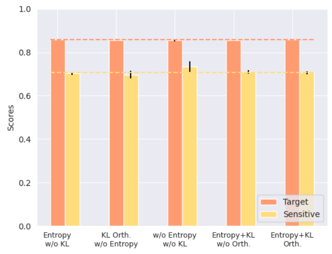

(b) Adult

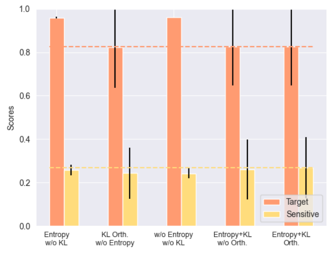

(c) CIFAR-10

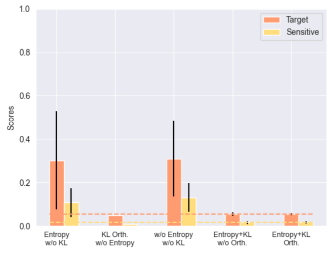

(d) CIFAR-100

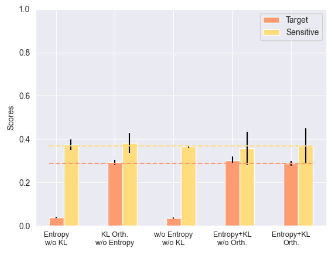

(e) YaleB

Figure 2: Target and sensitive accuracies of our model trained using various combinations of loss term components, results are averaged over 5 random seeds. Specifically, Entropy refers to the $\mathcal{L}_E$ component, Orth refers to the orthogonality constraint between the prior means, and KL refers to the $\mathcal{L}_{OD}$ component (c.f. Sarhan et al. [2020]).

Adult, YaleB, and German

Note that for the following results, we focus on the comparison between performances of the proposed models. We have included a comparison of the alternative models in Figure 1 mainly to be able to investigate discrepancies in our reimplementation outside of the proposed method itself (e.g. significant differences in the dataset definition, pre-processing, et cetera).

Our results for Adult, as displayed in Figure 1, are similar to those obtained by Sarhan et al. [2020], with the only difference being a small increase in our sensitive accuracy with regards to theirs. As for German, we observe similar, yet not identical, target and sensitive accuracies. We have to note that for runs during training with certain random seeds, a target accuracy was obtained that was identical to the 76% reported by Sarhan et al.; however, over multiple runs, we obtain a lower average accuracy around 73% (see Figure 1). For YaleB, we were not able to reproduce the accuracies reported by Sarhan et al. Instead, our model achieved a lower target accuracy, and a sensitive accuracy which is further away from the majority label classifier, suggesting that our model's performance was worse than that of Sarhan et al.

Ablative

The results of our ablative study are shown in Figure 2, which can be compared with the ablative study of Sarhan et al. in Figure in Appendix B. As a discussion of the potential implications of the various combinations explored in this ablative study forego the scope of this paper, we refer to Sarhan et al. [2020] for a detailed overview. The baseline measurement was omitted as it was unclear from the text what it entailed.

In comparison to Sarhan et al., for German, we see that varying loss components seems to have less impact on performance; for Adult, we see similar invariability for target accuracy but a lower impact on sensitive accuracy; for CIFAR-10, we observe a larger variance in performance over seeds and loss components; and lastly, CIFAR-100 and YaleB results are significantly different. In summary, our ablative study results generally do not exhibit the same patterns as those of Sarhan et al. This may, however, be attributed to our use of random seed averaging.

Sensitivity analysis on Adult

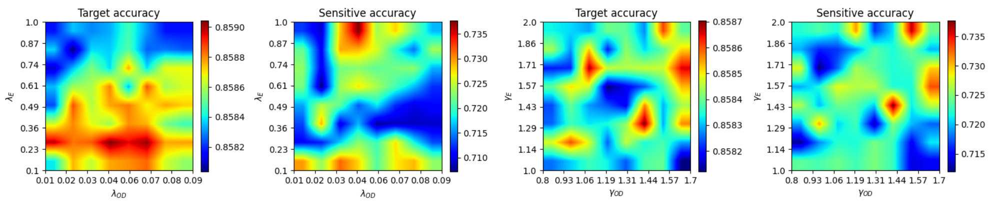

Figure 3: Target and sensitive accuracies when varying λ_{OD} together with λ_E (left), and when varying γ_{OD} together with γ_E (right).

The results of our sensitivity study are shown in Figure 3, which can be compared with the sensitivity study of Sarhan et al. in Figure in Appendix B.

When comparing these sensitivity analyses, it can easily be observed that there is very little in common between the two. First off, there is, for each subfigure, a sizeable difference in the accuracy ranges. This difference is in line with differences encountered in Figures 1a and 1d. More importantly, however, there is very little similarity to be found in any of the accuracy landscapes displayed, with peaks and valleys located in different places. In the reference sensitivity analysis, these landscapes are smooth. However, this is also not reflected in our sensitivity analysis. Note that the smoothness of the reference sensitivity analysis might be visually exaggerated due to a relatively low number of coordinate samples compared to ours.

5 Discussion

The claim of the original authors are as follows: by disentangling the latent representation of a data sample into two subspaces that are orthogonal to each other, as well as training the model using a loss function that encourages it to encode sensitive information into one of these subspaces, and meaningful information for the task at hand into the other of those subspaces, it is possible to create meaningful representations that do not contain any information from which a protected, or sensitive, attribute can be inferred.

In order for our results to support this claim, they would need to show that the proposed model is able to create representations that perform well on the target task (i.e. attains a high target accuracy), while it performs poorly in the inference of the sensitive attribute using the target representation (i.e. attains a sensitive accuracy close to the accuracy of majority voting). When looking at our results, we observe that this is indeed the case for the German dataset. However, for the Adult and CIFAR-10 datasets, the attained sensitive accuracy is substantially higher than the majority vote baseline; and for the CIFAR-100 and YaleB datasets, the model does not achieve a satisfactory performance in terms of target accuracy; and so, results from these four datasets do not appear to support the original claim of the authors. Likewise, those patterns that the authors observe in their ablative studies are reproduced in our own ablative studies.

This means that there is a discrepancy between our results and the original results from Sarhan et al. [2020]. Thus, when considering the large effort undertaken in this research to minutely re-implement their proposed method, we conclude that the original paper is relatively difficult to reproduce, and can in fact not be reproduced based solely on its contents.

5.1 What was easy

We experienced especially the theoretical part of the paper to be well structured and though out. The set-up of the two types of representations and notions of disentanglement and orthogonality makes sense intuitively. Additionally, all loss terms are well described and were therefore easy to implement.

5.2 What was difficult

Performance fluctuations and training instability One of the issues we ran into is that for these models training seems to be unstable, which is evident from the high fluctuation in performance when we vary the random seed or the number of maximum epochs. This is not addressed in the paper and therefore there is no information on how to deal with it. To add to this, it was unclear what trade-off between target and sensitive accuracy was used by the authors to select the best model during training. This trade-off ultimately determines which model is selected for testing which can have a large influence on performance.

Implementation There were a few unclear aspects of the model implementation that we resolved either by making a choice that seemed logical to us, or through contacting the original author. For example, there was limited information on how certain losses were backpropagated with a shared encoder network. Besides this, the implementation of the decay the two λ parameters was not clearly reported. These issues were both resolved in contact with the authors.

Hyperparameters The amount of epochs that the model was trained was not reported in either the paper or its supplementary material. This was quite an important value given that no explicit stopping criterion was mentioned either. In correspondence with Sarhan et al., we were able to set values for the `step_size` hyperparameter that correspond to those used by the original team. Furthermore, amongst the not reported hyperparameters were those involved the training of the network-based target and sensitive predictors. These include the optimizer used, the learning rate, weight decay, amount of epochs as well as the nonlinearities, to name a few.

Dataset details As mentioned in YaleB paragraph of the Datasets section we have made a number of assumptions about how to set up the classes corresponding to the sensitive attributes, which might have some influence on the performance of our approach for this datasets. We were unsure about some other details concerning the data as well. Namely, the type of data-normalization is not specified, and for the German dataset there is not a train-test split reported. However, these details were not as vital for reproduction as the aforementioned issue concerning the YaleB dataset.

5.3 Communication with original authors

We have had the pleasure of communicating with the original authors of the paper. This helped getting our hands on some additional hyperparameters, such as the stepsize t_s and the dimensions of the latent representations for some datasets, to name a few. Furthermore, we got insight in some implementation details, such as how the loss weights λ_{OS} and λ_E are updated and how the losses are backpropagated when dealing with a shared encoder network. The authors were going to give us extra information on the YaleB dataset specifically, but we were not able to receive said information in time.

5.4 Our approach

Due to the large scope of the research performed in our reference paper, our approach was diverse from the start. Many different avenues were explored from the beginning, dataloaders for all of the datasets were implemented and we had quickly written code to produce many of the figures necessary to asses the reproducibility of the research. While this meant that we gained a better understanding of the models' performance and behaviour on all of the datasets and tasks from the beginning, it was complicated to work on all the tasks and datasets simultaneously.

References

Mhd Hasan Sarhan, Nassir Navab, Abouzar Eslami, and Shadi Albarqouni. Fairness by learning orthogonal disentangled representations, 2020.

Qizhe Xie, Zihang Dai, Yulun Du, Eduard Hovy, and Graham Neubig. Controllable invariance through adversarial feature learning. *arXiv preprint arXiv:1705.11122*, 2017.

Proteek Chandan Roy and Vishnu Naresh Boddeti. Mitigating information leakage in image representations: A maximum entropy approach. In *Proceedings of the IEEE/CVF Conference on Computer Vision and Pattern Recognition*, pages 2586–2594, 2019a.

Novi Quadrianto, Viktoriia Sharmanska, and Oliver Thomas. Discovering fair representations in the data domain. In *Proceedings of the IEEE/CVF Conference on Computer Vision and Pattern Recognition*, pages 8227–8236, 2019.

Hardt M. Narayanan A. Barocas, S. Fairness and machine learning. fairml-book.org, 2019. URL `http://www.fairmlbook.org`.

Francesco Locatello, Gabriele Abbati, Tom Rainforth, Stefan Bauer, Bernhard Schölkopf, and Olivier Bachem. On the fairness of disentangled representations. *arXiv preprint arXiv:1905.13662*, 2019.

Diederik P Kingma and Max Welling. Auto-encoding variational bayes, 2014.

Diederik P Kingma and Max Welling. Auto-encoding variational bayes. *arXiv preprint arXiv:1312.6114*, 2013.

Dheeru Dua and Casey Graff. UCI machine learning repository, 2017. URL `http://archive.ics.uci.edu/ml`.

Athinodoros S Georghiades, Peter N Belhumeur, and David J Kriegman. From few to many: Generative models for recognition under variable pose and illumination. In *Proceedings fourth ieee international conference on automatic face and gesture recognition (cat. no. pr00580)*, pages 277–284. IEEE, 2000.

K.C. Lee, J. Ho, and D. Kriegman. Acquiring linear subspaces for face recognition under variable lighting. *IEEE Trans. Pattern Anal. Mach. Intelligence*, 27(5):684–698, 2005.

Christos Louizos, Kevin Swersky, Yujia Li, Max Welling, and Richard Zemel. The variational fair autoencoder. *arXiv preprint arXiv:1511.00830*, 2015.

Proteek Chandan Roy and Vishnu Naresh Boddeti. Mitigating information leakage in image representations: A maximum entropy approach. *CoRR*, abs/1904.05514, 2019b. URL `http://arxiv.org/abs/1904.05514`.

Kaiming He, Xiangyu Zhang, Shaoqing Ren, and Jian Sun. Identity mappings in deep residual networks. In *European conference on computer vision*, pages 630–645. Springer, 2016.

Diederik P Kingma and Jimmy Ba. Adam: A method for stochastic optimization. *arXiv preprint arXiv:1412.6980*, 2014.

Appendix

A Loss terms derivations

Representation loss

The representation target loss can be computed as follows:

$$\begin{aligned}\mathcal{L}_T(\theta_T, \phi_T) &= KL(p(\boldsymbol{y}|\boldsymbol{x}) \parallel q_{\phi_T}(\boldsymbol{y}|\boldsymbol{z}_T)) \\ &= -\sum_{\boldsymbol{y}} p(\boldsymbol{y}|\boldsymbol{x}) \log q_{\phi_T}(\boldsymbol{s}|\boldsymbol{z}_T) + \sum_{\boldsymbol{y}} p(\boldsymbol{y}|\boldsymbol{x}) \log p(\boldsymbol{y}|\boldsymbol{x})\end{aligned} \tag{7}$$

The second part of this expression solely depends on the true posterior of our data and hence does not depend on our neural network. Therefore, we drop it here. What remains is equal to the cross-entropy loss:

$$\mathcal{L}_T(\theta_T, \phi_T) = \sum_{\boldsymbol{y}} p(\boldsymbol{y}|\boldsymbol{x}) \log q_{\phi_T}(\boldsymbol{s}|\boldsymbol{z}_T) \tag{8}$$

This is the same as the cross-entropy loss over the output of the discriminator. The representation sensitive loss can be computed in similar fashion.

Maximum Entropy loss

We can compute the entropy loss as follows:

$$\begin{aligned}\mathcal{L}_E(\phi_S, \theta_T) &= KL(q_{\phi_S}(\boldsymbol{s}|\boldsymbol{z}_T) \parallel \mathcal{U}(\boldsymbol{s})) \\ &= \sum_{\boldsymbol{s}} q_{\phi_S}(\boldsymbol{s}|\boldsymbol{z}_T) \log q_{\phi_S}(\boldsymbol{s}|\boldsymbol{z}_T) - \sum_{\boldsymbol{s}} q_{\phi_S}(\boldsymbol{s}|\boldsymbol{z}_T) \log \mathcal{U}(\boldsymbol{s}) \\ &= \sum_{\boldsymbol{s}} q_{\phi_S}(\boldsymbol{s}|\boldsymbol{z}_T) \log q_{\phi_S}(\boldsymbol{s}|\boldsymbol{z}_T) - \log \frac{1}{m} \sum_{\boldsymbol{s}} q_{\phi_S}(\boldsymbol{s}|\boldsymbol{z}_T) \\ &= \sum_{\boldsymbol{s}} q_{\phi_S}(\boldsymbol{s}|\boldsymbol{z}_T) \log q_{\phi_S}(\boldsymbol{s}|\boldsymbol{z}_T) + \log m\end{aligned} \tag{9}$$

The second term is a constant and will be the same for every loss no matter the network, hence we drop it:

$$\mathcal{L}_E(\phi_S, \theta_T) = \sum_{\boldsymbol{s}} q_{\phi_S}(\boldsymbol{s}|\boldsymbol{z}_T) \log q_{\phi_S}(\boldsymbol{s}|\boldsymbol{z}_T) \tag{10}$$

Note that by dropping the last term, the entropy loss will always be negative.

Orthogonal-Disentangled loss

We can write out the OD target loss as follows,

$$\begin{aligned}\mathcal{L}_{\boldsymbol{z}_T}(\theta_T) &= KL(q_{\theta_T}(\boldsymbol{z}_T|\boldsymbol{x}) \parallel p(\boldsymbol{z}_T)) \\ &= -\sum_{i=1}^{d_T} KL(q_{\theta_T} z_T^i|\boldsymbol{x}) \parallel p(z_T^i))\end{aligned}$$

because both the prior and the encoder posterior are independent Gaussian distributions, the KL divergence between the two is simply a sum over KL divergences between the univariate Gaussians $q_{\theta_T}(z_T^i|\boldsymbol{x})$ and $p(z_T^i)$.

One KL divergence terms can be computed as follows:

$$\begin{aligned}KL(q_{\theta_T}(z_T^i|\boldsymbol{x}) \parallel p(z_T^i)) &= -\int q_{\theta_T}(z_T^i|\boldsymbol{x}) \log \frac{q_{\theta_T}(z_T^i|\boldsymbol{x})}{p(z_T^i)} d\boldsymbol{x} \\ &= \frac{1}{2}\log(2\pi\sigma_{p_T}^i) + \frac{(\sigma_{q_T}^i)^2(\mu_{q_T}^i - \mu_{p_T}^i)^2}{2(\sigma_{p_T}^i)^2} - \frac{1}{2}(1 + \log 2\pi(\sigma_{q_T}^i)^2) \\ &= \log\frac{\sigma_{p_T}^i}{\sigma_{q_T}^i} + \frac{(\sigma_{q_T}^i)^2(\mu_{q_T}^i - \mu_{p_T}^i)^2}{2(\sigma_{p_T}^i)^2} - \frac{1}{2}\end{aligned} \tag{11}$$

In practice, we will compute the element-wise KL divergence between the prior and posterior and sum over the result. The OD losses therefore require the output *means* and *variances* of the encoder network and the *prior distributions* of the latent variable. The OD sensitive loss can be computed in a similar way.

B Dataset details

Table 3: Details concerning the several datasets we used. Here MV target and MV sensitive correspond to how much percent of the data belongs to the biggest target and sensitive class respectively. The input size corresponds to the amount of features in the case of the tabular data and for the picture dimensions of the visual data.

	sample amount	train/test split	input size	MV target	MV sensitive
Adult	$48,842$	2 : 1	108	75%	67%
German	1000	4 : 1	61	68%	70%
YaleB	2433	190 : 2243	192×168	2.7%	35.6%
CIFAR-10	$60,000$	5 : 1	$3 \times 32 \times 32$	60%	10%
CIFAR-100	$60,000$	5 : 1	$3 \times 32 \times 32$	5%	1%

YaleB pre-processing

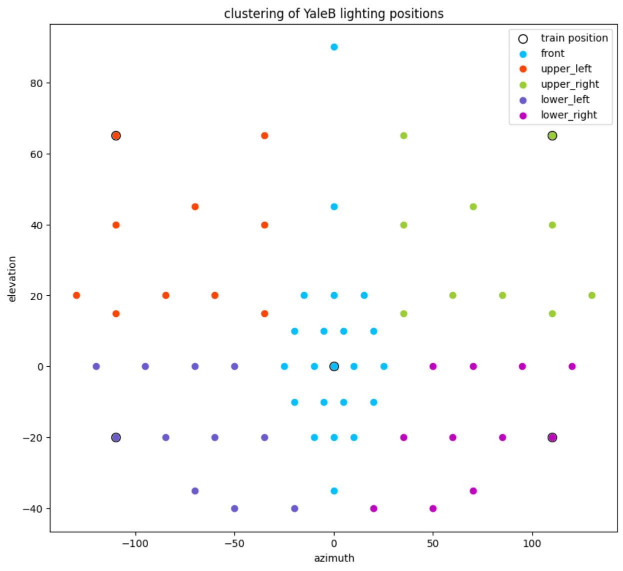

Figure 4: Definitions of YaleB sensitive attributes, which are a clustering of lighting positions, which are defined by an elevation and an azimuth.

In order to construct the sensitive attributes for the YaleB dataset, we define a five-class clustering for the lighting positions, which corresponds to a five-class sensitive attribute. These clusters, as well as the lighting positions that are selected for the train partition, are displayed in Figure 4.

C Hyperparameters

The hyperparameters that we used for our reported results can be found in table 4 and 5. Note that for all experiments we used the Adam optimizer [Kingma and Ba, 2014]. We should check whether these are in fact the last hyperparameters we used

Table 4: Hyperparameters that we used in our experiments for the various datasets. For the CIFAR datasets, the first number of the learning rate and weight decays refers to the encoder network and the second to the discriminator network.

	Learning Rate	Weight Decay	Batch Size	Max. Epochs
Adult	10^{-3}	5×10^{-4}	64	2
German	10^{-3}	5×10^{-4}	64	15
YaleB	10^{-4}	5×10^{-2}	64	30
CIFAR-10	$10^{-4}, 10^{-2}$	$10^{-2}, 10^{-3}$	128	30
CIFAR-100	$10^{-4}, 10^{-2}$	$10^{-2}, 10^{-3}$	128	80

Table 5: The $\lambda_{OD}, \lambda_E, \gamma_{OD}$ and γ_E used for every dataset.

	λ_{OD}	λ_E	γ_{OD}	γ_E
Adult	0.037	0.55	0.8	1.66
German	0.01	1.0	1.4	2.0
YaleB	0.037	1.0	1.1	2.0
CIFAR-10	0.063	1.0	1.7	1.0
CIFAR-100	0.0325	0.1	1.2	1.67

D Encoder and Discriminator details

Table 6: Encoder and discriminator implementation details.

	Encoder			Discriminator	
	Network Type	Hidden Dims	Latent Dim	Network type	Hidden Dims
Tabular	MLP	64	2	MLP	64, 64
YaleB	MLP	100	100	MLP	100, 100
CIFAR	ResNet-18	-	128	MLP	256, 128

D Target predictor details

We have reported the architectures and hyperparameters of the target predictor networks in Table 7. We used the Adam optimizer [Kingma and Ba, 2014] to optimize all MLP based predictor networks.

Table 7: Details of the target predictor network per dataset.

	Network Type	Hidden Dims	Learning Rate	Weight Decay
Tabular	Logistic Regression	-	-	-
YaleB	MLP	100	10^{-3}	0
CIFAR	MLP	256, 128	10^{-3}	0

E Ablative and sensitive study results in Sarhan et al. (2020)

For ease of comparison, we include two Figures from the reference paper. All rights for Figures and reserved by Sarhan et al.

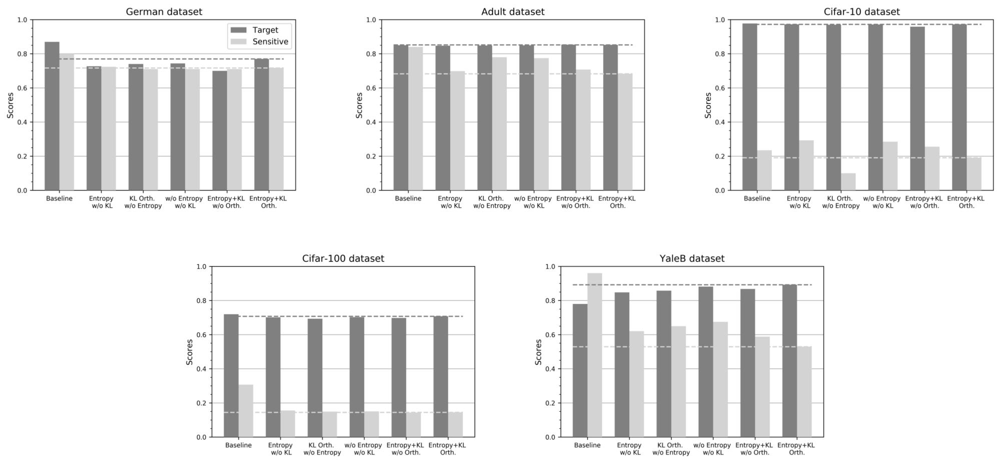

Figure 5: Figure 3 from Sarhan et al. [2020], with original caption: *Ablative study. Dark gray and light gray dashed lines represent the accuracy results on the target and sensitive task respectively for the "Entropy + KL Orth." model.*

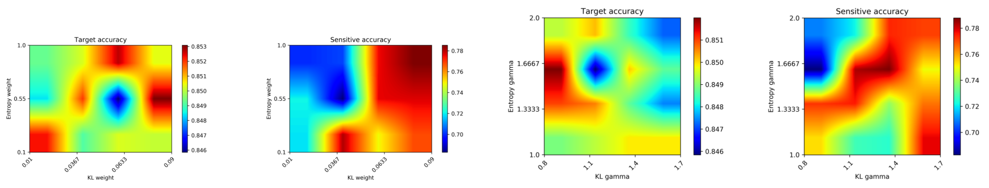

Figure 6: Figure 5 from Sarhan et al. [2020], with original caption: *Sensitivity analysis on the Adult dataset*